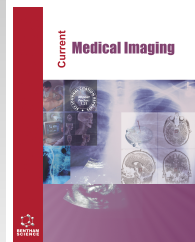




Current Medical Imaging

Content list available at: <https://benthamscience.com/journals/cmim>



SYSTEMATIC REVIEW

Machine Learning in Magnetic Resonance Images of Glioblastoma: A Review

Georgina Waldo-Benítez¹, Luis Carlos Padierna¹, Pablo Cerón² and Modesto A. Sosa^{1*}

¹División de Ciencias de Ingenierías, Universidad de Guanajuato, León, 37150, México

²Universidad de Quintana Roo, División de Ciencias, Ingeniería y Tecnología, Chetumal, 77019, México

Abstract:

Background:

The purpose of this work was to identify which Glioblastoma (GBM) problems can be handled by Magnetic Resonance Imaging (MRI) and Machine Learning (ML) techniques. Results, limitations, and trends through a review of the scientific literature in the last 5 years were performed. Google Scholar, PubMed, Elsevier databases, and forward and backward citations were used for searching articles applying ML techniques in GBM. The 50 most relevant papers fulfilling the selection criteria were deeply analyzed. The PRISMA statement was followed to structure our report.

Methods:

A partial taxonomy of the GBM problems tackled with ML methods was formulated with 15 subcategories grouped into four categories: extraction of characteristics from tumoral regions, differentiation, characterization, and problems based on genetics.

Results:

The dominant techniques in solving these problems are: Radiomics for feature extraction, Least Absolute Shrinkage and Selection Operator for feature selection, Support Vector Machines and Random Forest for classification, and Convolutional Neural Networks for characterization. A noticeable trend is that the application of Deep Learning on GBM problems is growing exponentially. The main limitations of ML methods are their interpretability and generalization.

Conclusion:

The diagnosis, treatment, and characterization of GBM have advanced with the aid of ML methods and MRI data, and this improvement is expected to continue. ML methods are effective in solving GBM-related problems with different precisions, Overall Survival being the hardest problem to solve with accuracies ranging from 57%-71%, and GBM differentiation the one with the highest accuracy ranging from 80%-97%.

Keywords: Artificial intelligence, Deep learning, Glioblastoma, Overall survival, Machine learning, Magnetic resonance imaging.

Article History

Received: June 29, 2023

Revised: August 18, 2023

Accepted: September 25, 2023

1. INTRODUCTION

Current research using Machine Learning (ML) for the analysis of clinical pathologies has addressed issues such as the diagnosis of metastases in lymph nodes [1], mechanical evaluation and sedative dose in the area of intensive care [2], image acquisition, segmentation and diagnosis for COVID-19 [3], for protein-protein interaction [4], and the prediction of patient attendance at medical appointments [5] and several others [6 - 9]. In medical physics, a joint subspecialty of

physics and medicine, applications of ML have considered cancer as a main object of study, and due to the substantial number of published articles, efforts have been made to review, organize, and classify ML methods and their applications to solve problems related to different types of cancers. For example, in breast cancer, ML techniques have been used for the classification of breast pathologies [10], prediction of the possible recurrence [11], selection of the best treatment [12] and prediction of the response to neoadjuvant cancer treatment [13]. Regarding lung cancer, ML has been used to research local tumor control [14] and automated radiation adaptation [15]. For other types of cancers, the prediction of biochemical

* Address correspondence to this author at the División de Ciencias de Ingenierías, Universidad de Guanajuato, León, 37150, México;
E-mail: modesto@fisica.ugto.mx

malfunction in irradiated patients with prostate cancer has been studied [16], as well as clinical decision support of radiotherapy treatment planning [17]. Likewise, improvement of automatic segmentation in the organs of the head and neck [18] liver [19] and esophagus [20] has been reported. Other works include the automatic segmentation of cardiac structures in radiotherapy [21], analyzes to predict the pain of the chest wall [22], and the survival in bladder cancer patients [23].

Glioblastoma (GBM) is an aggressive brain cancer in which, despite the development of new diagnostic tools and innovative therapies, no improvement in the patient's health has been shown [24]. Previous reviews on the intersection between ML and GBM are scarce and focus on describing the technical aspects of ML algorithms instead of analyzing the related GBM problems [25] or on the revision of specific GBM subproblems such as the differentiation of GBM from Primary Central Nervous System Lymphoma (PCNSL) [26], the assessment of metabolic markers in GBM [27], the imaging biomarkers of GBM treatment response [28] or the survival prediction of GBM patients [29]. Therefore, it remains unclear which GBM problems and subproblems have been addressed with ML, the results obtained so far, and the future trends of this paradigm.

The objectives of this work are, first, to identify the problems associated with GBM handled with ML in the last 5 years (2018-2022) and to propose a partial taxonomy of these problems and subproblems; second, to describe a broad range of applications for different purposes in the study of GBM; and third, to collect the most successful methods used in the literature. We aim to reach a public with basic knowledge about GBM, ML, or both fields, interested in obtaining updated and structured information regarding the latest advances and solutions provided by ML for GBM.

For the sake of brevity and to avoid duplicating theoretical information reported in previous reviews, technical formulations of the ML methods are omitted. Instead, a set of two papers explaining the most common algorithms in ML [30], and specifically, Artificial Neural Networks (ANN) [31] are provided. Section 2 describes the methodology for our review based on the PRISMA guidance. Section 3 shows the state of the literature on the intersection between ML and GBM. In section 4, a discussion of the main findings, a taxonomy of the ML methods employed, their usage per year, limitations and trends are presented. Lastly, relevant conclusions are presented in section 5.

2. MATERIALS AND METHODS

2.1. Information Sources

During June 2021 – March 2023, Google Scholar, PubMed, Elsevier databases, and forward and backward citations were used to search articles applying ML techniques in MRI for GBM. 9,399 manuscripts from the last 15 years were retrieved, 7,982 from the last five years, and 50 were finally evaluated with the following eligibility criteria, roughly 10 per year.

2.2. Eligibility Criteria

Articles that include in their title or abstract the keywords GBM, Machine Learning, Deep Learning (DL), and MRI were selected and classified considering six criteria: (1) investigation or application area, (2) method type, (3) language, (4) publication type, (5) publication date and (6) citation. For the application area, articles solving a GBM-related problem were included. Pure statistical methods were discarded and only articles experimenting with ML methods were incorporated. Articles written in a language different from English were not included. Publications appearing in indexed journals were included, but conferences, patents, and other sources were not considered.

2.3. Search Strategy

The keywords used in the search tools of the considered databases were: “Glioblastoma + Machine Learning + MRI” and “Glioblastoma + Deep Learning + MRI”. Relevant articles were retrieved with filters that sorted all the articles fulfilling the criteria and selected those with the highest number of citations.

2.4. Selection and Data Collection Process

For each article, the following information was extracted: title, abstract, date, authors, country, journal, citation, objective, ML/DL methods, MRI technique, the best quantitative results, and conclusion. Mendeley® and Notion® software were used to systematically arrange relevant articles. All those papers that reported performance indexes above or below the average were double-checked by a different pair of reviewers to ensure that the methodology was correct, and thus avoiding bias.

2.5. Data Items

We included 50 relevant articles that fulfill all eligibility criteria of the last 5 years (2018-2022), on studies using ML techniques applied to GBM. Although publications in the last 15 years were searched, we limited the analysis to the last 5 years because the majority of published articles are in this period, as shown in Fig. (1).

3. RESULTS

The PRISMA flowchart shown in Fig. (2) illustrates the procedure for selecting scientific articles on GMB problems solved by ML methods. The first search retrieved 9,399 manuscripts. Then, by applying filters on the year and the article type, and excluding repeated articles or non-relevant ones, we selected the 50 more relevant papers on which all the following results are based.

One of the main results of this review is the proposal of a partial taxonomy in which the different GBM subproblems can be classified into the following four categories: feature extraction, differentiation, characterization, and genetics-based problems. These categories and 15 subcategories are illustrated in Fig. (3) and described in the next sections. Each section and subsection starts with a brief introduction to the GBM-related problem, then a description of the task or tasks associated with

the problem, the ML methods, the performance achieved, and a clinical interpretation is provided for each of the analyzed articles.

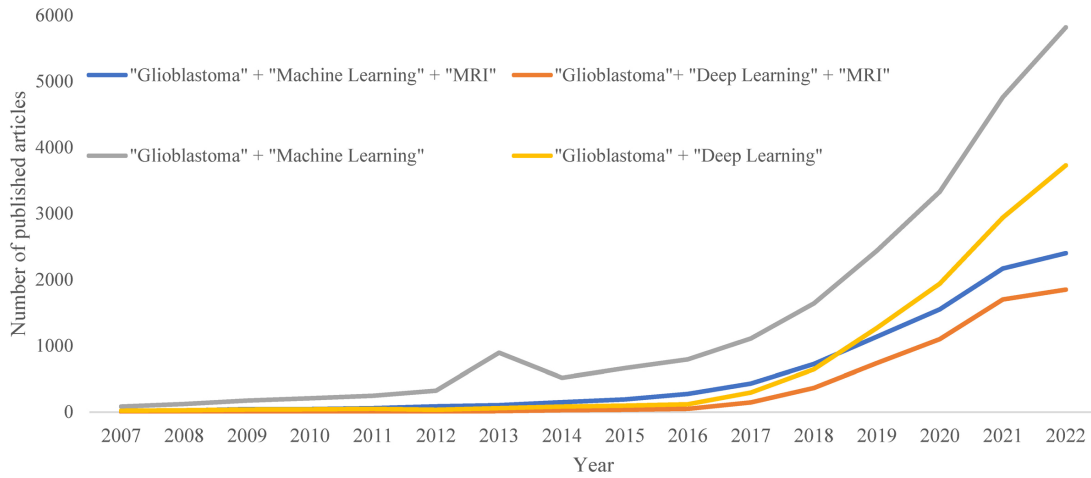


Fig. (1). Papers published in the last 15 years related to Glioblastoma and Machine Learning. A growing trend in the articles applying Machine Learning techniques to Glioblastoma in the last 10 years, and in the last 5 years applying Deep Learning is observed.

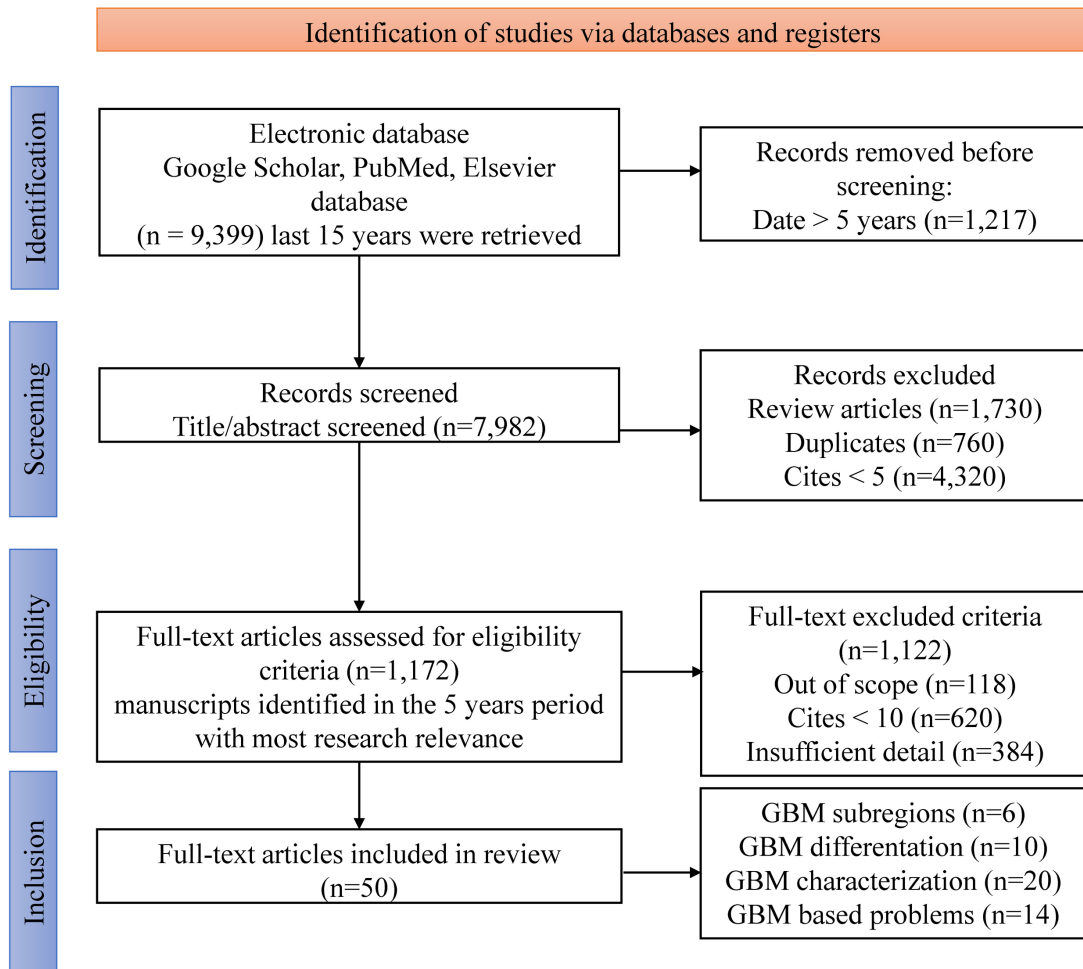


Fig. (2). Flowchart that describes the search and selection process of the papers.

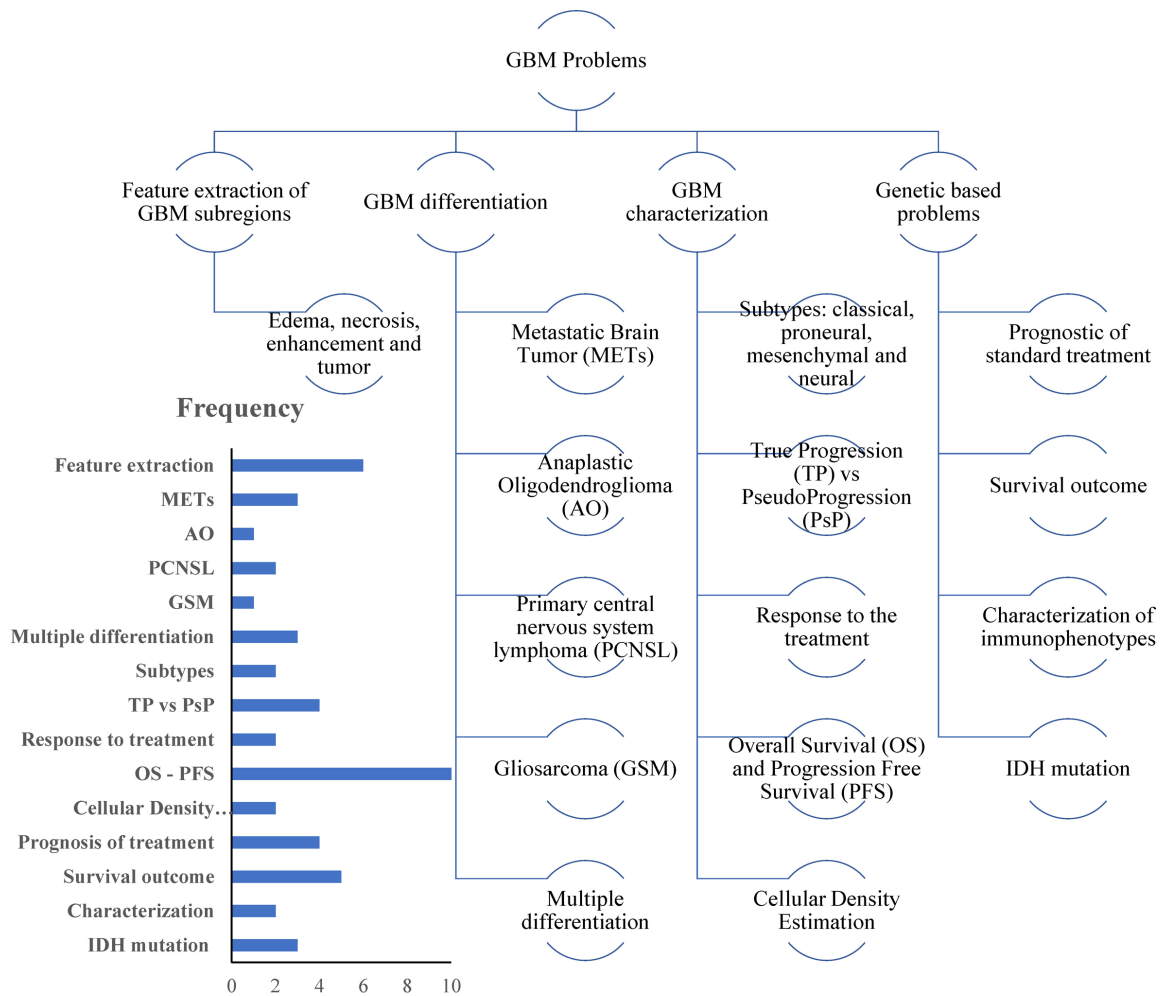


Fig. (3). Partial taxonomy of problems related to GBM tackled with ML Methods. GBM subproblems appeared with different frequencies, and this is indicated with bars. In general, from the four types of problems that were identified, the characterization of GBM and the problems based on genetics were more addressed than feature extraction and GBM differentiation. Within all the subproblems, the analysis of OS is the most studied, followed by feature extraction and survival outcome.

3.1. Feature Extraction of GBM Subregions (Edema, Necrosis, Enhancement, and Tumor)

There are specific regions in GBM such as edema (swelling of the brain), necrosis (permanent death of the brain tissue), enhancement (an abnormal radiologic sign obtained using radiocontrast), and tumor (mass of abnormal cells), that have been studied to find relationships with the evolution of the patient [32, 33]. We can extract the main characteristics of these regions by using radiomics, which is a quantitative approach to medical imaging in radiology and oncology, where high-throughput features related to the shape of the tumor, the grey levels of the image, the first, second, and higher orders statistics are used to measure underlying correlations of the tumor phenotype with the information in the image that cannot be obtained by the naked eye of the expert [34 - 36]. These characteristics are the base for developing models that describe the growth, evolution, and prognosis of GBM. The radiomics method also allows for finding relationships between imaging attributes and biological or clinical features. From the four GBM regions, the reproducibility of features extracted by radiomics was more stable and less sensitive to the intensity

inhomogeneities and noise, in necrosis compared to edema, enhanced, and active-tumor regions, on different imaging preprocessing [37].

Machine Learning models designed after radiomics feature extraction have solved different GBM-related problems, such as Overall Survival (OS), segmentation, the measure of concentrations, survival classification, and others. To predict short-term survival (less than 6 months) in GBM patients a radiomic feature extraction of structural preoperative multiparametric MRI (mpMRI) was performed [38]. The Naïve-Bayes [39] algorithm reached an accuracy of 80% in this task with patients who underwent total or near-total resection of the enhancing tumor. A remarkable relationship between the amount of resection and short-term survival was observed. For the segmentation task in edema, enhancing, and necrosis subregions, a Convolutional Neural Network (CNN) named U-Net [40] was used. The resulting segmentation along with other clinical features was able to predict the OS for three survival groups, short, medium, and long, through an XGBoost [41] algorithm which reached an accuracy of 0.73 [42]. The performance of both Naïve-Bayes and XGBoost is low for OS

prediction due to the complexity of this GBM-related problem.

Another problem is to measure concentrations of areas of high cellularity, tumor infiltration, and tumor necrosis; a Support Vector Machine (SVM) [43] classifier and Diffusion Histology Imaging were employed to solve this problem, reaching accuracies of 87.5%, 93.4%, and 89.0%, respectively [44]. This result suggests Diffusion Histology Imaging as an alternative to available techniques of neuroimaging for guiding biopsy, surgery, and following up the therapeutic response in the GBM treatment. Features extracted by radiomics from the enhancement of the tumor core, the non-enhancing portion of the tumor, and peritumoral edema subregions, helped to find an optimal radiomics nomogram where a Least Absolute Shrinkage and Selection Operator (LASSO) [45] algorithm and Cox survival model were used to select the most relevant features. This shows that combining multiple radiomics signatures derived from these subregions improves the survival prediction of patients compared to clinic and single region nomograms (C-index: training/test cohort from 0.656/0.535 to 0.717/0.655) [46]. This improvement seems marginal, but for survival prediction any increment in accuracy is important.

Defining the boundaries between the active tumor area and perifocal edematous extension is fundamental to radiotherapy and GBM resection. A combination of MRI-based radiomics and Random Forest (RF) [47] was an efficient classifier of tumor subregions of GBM in [48] where it was found that prognostic radiomic features, extracted from necrosis, solid part, edema, and peritumoral tissue regions from MRI exams are correlated with biological processes influencing the response to chemotherapy. The classification accuracies were 93.6% for necrosis, 90.4% for the solid part, 95.8% for peritumoral tissue, and 90.4% for peritumoral edema. This result means that the peritumoral features are useful for the diagnosis and segmentation of GBM. Chiu *et al.* [49] provided a qualitative image interpretation in GBM subregions and radiomics features in quantitative usage of image analysis, as well as ratios of these tumor components, to underlie the biological process and prognostic status of patients with GBM. The regions of a necrotic core, solid part, peritumoral tissue, and edema were considered. An RF for tumor subregions classification of GBM reached an accuracy of 95.8% in peritumoral tissue. An association between volumetric features and several sets of tumor phenotype features and biological processes was found.

The before-mentioned problems were addressed by ML methods trained with MRI data, which are difficult to obtain. Recently, the University of Pennsylvania [50] developed the largest publicly available collection of 630 patients diagnosed with GBM. This collection implemented expert annotations of tumor subregions and radiomic features corresponding to each region. The considered subregions were the enhancing tumor, the necrotic tumor core, and the peritumoral edematous/infiltrated tissue. This dataset is relevant because it allows us to train the ML models previously described and others, which focus on solving problems like segmentation, the measure of concentrations, survival classification, *etc.*

3.2. GBM Differentiation

The GBM diagnostic is usually performed through MR images, with which oncologists can establish the type of problem the patient faces; however, there are other pathologies such as Metastatic Brain Tumor (METs), Anaplastic Oligodendroglioma (AO), PCNSL or Meningioma, which can resemble GBM and confuses the expert. Studies applying ML techniques have helped to differentiate GBM from these diseases and to initiate appropriate treatment management according to the type of brain tumor.

3.2.1. Metastatic Brain Tumor

GBM and METs have similar MR imaging features. GBM presents a particular growth pattern, making the tumor cells disseminate further than the enhancing portion, which reveals a perilesional T2 hyperintense area. In METs, this hyperintensity can be a consequence of vasogenic edema. A DL-based model, ResNet-50, was used for differentiation between GBM and METs employing MRI, with an Area Under the Curve (AUC) of 0.89 and 0.83 in the internal and external tests [51]. Similarly, to differentiate between METs and GB a combination of 43 radiomic features, Distance Correlation as a feature selector, and Logistic Regression (LR) [52] as a classifier was implemented and obtained an accuracy of 80%. This model provided evidence that GBM commonly expands by infiltration, while METs grow by expansion [53]. The differentiation of GBM from METs preoperatively was performed with SVM and LASSO methods, reaching an AUC of 0.90 [54]. In this latter work, relevant radiomics attributes of the tumor microstructure were obtained, but not the attributes of different histology subtypes. The sphericity of the tumor has been proposed as a relevant characteristic to distinguish between GBM and METs [55].

3.2.2. Anaplastic Oligodendroglioma

As stated in the World Health Organization (WHO) taxonomy, AO is in Grade III, and GBM is in Grade IV derived from histological attributes. The standardized therapy for GBM after surgery is brain radiotherapy and temozolomide (TMZ) followed by adjuvant chemotherapy. For AO, it is advised to employ maximal resection followed by radiotherapy with adjuvant chemotherapy, in some cases clinical trial is recommended. AO has been confused with GBM in human readers' radiological evaluations. An ML model was proposed [56] to discriminate between these two diseases. For this classification task, filter algorithms like Gradient Boost Decision Tree (GBDT) [57] and LASSO with the combination of SVM and Linear Discriminant Analysis (LDA) [58] classifiers were used, achieving an AUC of 0.986. This could be useful in routine clinical practice to improve GBM and AO differentiation.

3.2.3. Primary Central Nervous System Lymphoma

A higher degree of cellularity and permeable neo-vascularization are presented in PCNSL more frequently than in GBM. Misdiagnosis could occur due to the images of atypical GBM and PCNSL being hard to differentiate. MRI radiomics and other ML algorithms discriminated GBM from

PCNSL with high accuracy, SVM with 96.4%, and LDA with 97.9% [59]. In this study, it was also found that heterogenous enhancement appeared more frequently in GBM cases (98%) than the homogenous enhancement in PCNSL cases (64%); in GBM, necrosis was presented in 88% of the cases, and only 5.6% in PCNSL. The differentiation of GBM and PCNSL without tumor delimitation was tackled with a CNN. The CNN was compared against senior specialist radiologists, reporting an accuracy of 89% and 90%, respectively, this indicates that CNN using images without tumor delimitation could be implemented in the clinical area [60].

3.2.4. Gliosarcoma

Gliosarcoma (GSM) is a variant of GBM associated with a higher ratio of extracranial metastasis, and lower ratios of epidermal growth factor receptor (EGFR) and O6-Methylguanine-DNA Methyltransferase (MGMT) without Isocitrate dehydrogenase (IDH) mutations. These differences between GSM and GBM justify the need for a different treatment. In a study [61], an ML radiomics-based method extracted features from tumor mass and peritumoral edema to differentiate GBM from GSM. A LASSO + SVM algorithm obtained an AUC = 0.85. Tumor mass features significantly outperformed peritumoral edema features in this task ($P < 0.05$).

3.2.5. Multiple Differentiation

GBM differentiation not only has been performed against a unique contrast-enhancing brain tumor but also a multiclass approach has been considered to discriminate between GBM and more than one brain tumor at a time. In a study [62], a multistep scheme involving pre-processing, region of interest definition, feature extraction, and selection, and finally a classification step, was followed to differentiate GBM from METs, PCNSL, and meningiomas. The ML model employed was SVM which achieved an accuracy of 95.7% for GBM, 92.7% for metastasis, 97% for meningioma, and 91.5% for PCNSL. Very recently, another multiclass ML model along with physiological MRI, a technique that enables the quantitative assessment of microvascular architecture, neovascularization, oxygen metabolism, and tissue hypoxia, was applied to classify contrast-enhancing brain tumors: GBM, METs, AO, PCNSL, and meningioma, where RF was the ML model that obtained an accuracy slightly superior to radiologists, 0.875 vs. 0.850, respectively [63]. The classification of GBM, METs, and PCNSL preoperatively from MRI images indicates that neovascularization is not a distinctive feature of PCNSL, which has lower microvascular density. This was possible by employing a Multilayer Perceptron (MLP) [64] with VpNET2 tumor volumes, reaching an accuracy of 69.2% [65].

3.3. GBM Characterization

Once it is certain that we are working with GBM, there are other problems such as the classification of the different subtypes, the differentiation between Tumor Progression (TP) or Pseudoprogression (PsP), response to the treatment, and survival time. Each of these problems has been addressed by MRI and the ML methods described below.

3.3.1. Subtypes: Classical, Proneural, Mesenchymal, and Neural

The intensity, volume, and texture features from the tumor subregions aid in identifying associations with the proneural, mesenchymal, and classical GBM subtypes. Extracted radiomics features, including fractal dimensions of the necrosis, whole tumor, and tumor core regions were employed to make a pairwise classification problem, along with ML algorithms for differentiation of GBM subtypes, where SVM reached an accuracy of 62.7% for mesenchymal, 85.3% for classical and 81.82% for proneural [66]. Comparably, an XGBoost-based radiomics model, where 13 relevant features extracted from three subregions were employed to classify GBM subtypes, obtaining accuracies in the prediction of 71% for classical, 73% for mesenchymal, and 88% for both neural and proneural [67], this suggests that the incorporation of radiomic features to either XGBoost or SVM algorithm improves accuracy in discrimination of GBM subtypes.

3.3.2. True Progression vs Pseudoprogression

Pseudoprogression (PsP) can be defined as subacute radiographic changes within the radiation field, mimicking True Progression (TP). PsP needs to be differentiated from TP because disease management is completely different. In PsP, the patient is considered stable, but in TP, a treatment adjustment is necessary [68]. An analysis using mpMRI along with ML showed characteristic noninvasive signatures of TP vs PsP after GBM treatment. TP patients showed imaging characteristics with superior cellularity, angiogenesis, and lower water concentration compared to patients with PsP. A pre-trained CNN, ImageNet LSVRC-2010, was used for segmentation and feature extraction, adding an SVM to predict TP with an accuracy of 84% and 87% for PsP [69]. A different study developed a radiomics model from T1-weighted contrast-enhanced imaging after the standard GBM treatment. The RF algorithm was used to classify PsP and TP, finding that the tumor side along with the location of the tumor between these two groups were statistically significant. This model achieved an accuracy of 72.78% vs 66.23% from the radiologists [70].

The GBM progression phenotype was predicted using imaging analysis, ANN, and MR radiomics before surgery. The DL architectures VGG-16, ResNet-50, and a Decision Tree (DT) [71] were used to predict the progression in one of two classes, localized or diffuse; DT achieved an accuracy of 81% while ResNet50 and VGG16, 93.1% and 96.1% respectively, where worse OS prognosis was shown for the diffuse progression pattern in contrast with the distal progression that obtains better OS [72]. Considering patients labeled as PsP or TP based on histological diagnosis, a 3-D Densenet121 model was developed to differentiate between these two categories [73]. This architecture achieved an accuracy of 76.4%, however, further improvements must be made before its implementation in the clinical environment.

3.3.3. Response to the Treatment

The analysis of genetic, histological, and radiomic characteristics of patients with favorable responses to TMZ treatment allows us to offer the most appropriate treatment to

new patients. A retrospective study involved patients treated with TMZ, which were divided into response or non-response groups [74]. A binary classification problem considering these two groups was formulated and the highest accuracy was achieved by a tree-based algorithm with an AUC of 67%. Tree-based models are useful due to their high interpretability, which is essential in the clinical environment, however, the low AUC indicates that there is still room for improvement and other ML classifiers might be used, even if this produces a trade-off between interpretability and precision.

In addition to the response or non-response problem, ML techniques have stratified a group of patients by age [75]. Using MRI radiomic features along with unsupervised hierarchical clustering, it was found that there is a statistical significance between these age groups (T-test, p-value = 0.006) and that there is an age-related stratification with completely different genetic roots, suggesting that treatment must be different in the younger and elder population.

3.3.4. Overall Survival Time – Progression-free Survival

Overall survival (OS) is the time from the date of diagnosis until the day on which patients are still alive. On the other hand, progression-free survival (PFS) is the time when the disease does not get worse [76]. The combination of MRI features, genetic profiles, and clinical data has improved the performance of ML models addressing OS and PFS prediction. Radiomic features extracted from multiparametric MRI, genetic profiles (IDH1 and MGMT), and clinical data like age, Karnofsky Performance Status, resection extent, and postoperative treatment were combined in a Random Survival Forest, which is an ensemble of tree-based algorithms that ensures that individual trees are de-correlated [77]. This model was used to predict OS and PFS, achieving an AUC of 0.652 and 0.590, respectively. MR images and clinical records of GBM patients who have received surgery and concurrent chemoradiotherapy were the input for a CNN-based DL model that predicts OS time as a continuous variable [78]. This model showed a C-index of 0.768 and an integrated AUC of 0.790, indicating that using both clinical and radiomic parameters is useful for OS prediction. Similarly, MRI images for predicting GBM from brain tumors are implemented in a dynamic architecture of Multilevel Layer modeling in Faster R-CNN (MLL-CNN) for the classification of total survival. The proposed method produces an average accuracy of 95% in OS prediction [79].

Another approach to OS prediction considered patient stratification into short, medium, and long survivors. Radiomic features extracted from three tumor subregions on standardized pre-operative mpMRI and an ensemble learning model, random subspace discriminant, achieved an accuracy of 57.8% in predicting these three survival classes [80]. This low performance indicates the hardness of the OS prediction problem, and consequently, the need for more experimentation with ML models. Following the stratification approach, the CNN VGG-19 was employed to discriminate between long- and short-term survivors with a log-rank test-p value of 0.014 [81]. Also, a radiomics nomogram for preoperative prediction of survival stratification in GBM patients was constructed [82].

They used features extracted from mpMRI and SVM for classification obtaining AUCs of 0.877 and 0.919 in the training and validation cohorts, respectively. This non-invasive tool could facilitate clinical decision-making for preoperative prediction. In a complementary research line, patient survival and its association with biomarkers extracted from MRI images in GBM and clinical features were studied [83]. Using ML algorithms like ANN, C5, Bayesian, and Cox models to determine the most relevant biomarkers, an accuracy of 70.55% was achieved. Here, it was found that the largest size of width, largest size of length, and age are biomarkers associated with a patient's survival. Other works related to survival prediction, generated radiomic signatures for OS prediction [84], predicted 6 months postoperative Karnofsky Performance Status [85], and differentiated short-term from long-term survival patients based on the Resting State Functional Connectivity [86].

3.3.5. Cellular Density Estimation

Increased cellular density is a characteristic of gliomas, both in the bulk of the tumor and in areas of tumor infiltration into the surrounding brain. Making quantitative and spatially specific estimates of cellular density, through MR imaging techniques, is an important task to benefit patients. Relevant clinical applications include surgical guidance for the extent of resection and dosimetric radiation targeting of non-enhancing residual tumor during postoperative adjuvant care. An MR imaging-based transfer learning approach is proposed [87] to optimize individualized models of tumor cell density (TCD) and extent for patients with GBM. These models show high predictive performance ($r = 0.88$, mean absolute error = 5.66%), which indicates that TCD is significantly correlated with the non-enhancing infiltrative tumor segment. This tumor segment is problematic for the diagnosis and treatment of GBM. TCD was also estimated in a study [88] with moderate-to-strong correlations using MR imaging inputs and the RF algorithm, obtaining an $R^2 = 0.59$ between predicted and observed values.

3.4. Genetic-based Problems

The genetic information of GBM is a valuable tool for its study and classification. This information helps to solve different problems, ranging from knowing the prognosis for each type of treatment, survival results, characterization of immunophenotypes, and the outcome of patients with IDH1 mutation, among others. The solution to these problems improves the choice of treatment, shows the factors that can influence the recovery of the patient, and allows a better therapeutic follow-up. In addition to IDH1, other genes such as MGMT and EREG have been of interest to researchers in the GBM study. The use of gene expression in an initial diagnosis can contribute to the selection of treatment and survival prognosis. However, not all hospitals can obtain histologic information because it involves both an extra cost and an invasive procedure. Thus, it is necessary to find relationships between the images and the genetic expressions of the tumor.

3.4.1. Prognostic of Treatment Response

Depending on the first diagnosis using tumor gene

expression, the prognostic potential for a GBM patient's survival that has received standard treatment may change. A survival prediction model to recognize genes that might be therapeutic targets or biomarkers was implemented by using a deep MLP network with a Rectifier Linear Unit (ReLU) function [89]. From this, the top 10 ranked genes related to GBM stem cells, stem cell niche environment, and treatment resistance mechanisms were found, with a concordance index of 0.70 ± 0.07 . Another genetic-based problem consists in finding the hierarchical structure from data on cancer gene expression, and thus, understanding the cellular signaling. An unsupervised DL model (deep belief network) was developed, obtaining a Kaplan-Meier p-value of 0.002. Their consensus clustering led to the discovery of GBM clusters with differential survival. The expressed genes and mutations like NF1, IDH1, and EGFR were uniquely correlated with each of these clusters [90]. MGMT gene methylation status is a predictive biomarker for TMZ treatment resistance and poor PFS. This characteristic is difficult to obtain due to the high prices for detection and the complexity of the tumor. A model to predict between methylated and unmethylated classes was proposed [91], who employed a radiomics-based ML model for feature extraction, followed by a Genetic Algorithm-based wrapper for feature selection, and the XGBoost classifier with which an accuracy of 92.5% was achieved. Pretreatment prediction of MGMT was considered [92], where predictive models combining clinical factors and, six-feature radiomics were employed, showing an accuracy of 80% and suggesting that this may be a potential imaging biomarker for pretreatment of MGMT methylation.

3.4.2. Survival Outcome

Using mpMRI images, radiomics features were extracted from multi-habitats of the tumor and used as an imaging biomarker. GBM patients were successfully stratified using consensus clustering revealing inherent phenotypic subtypes, "heterogenous enhancing", "rim-enhancing necrotic", and "cystic", where each one of these, represents a worst, intermediate, and favorable prognosis, respectively, with a p-value = 0.003 between these groups [93]. Extractions from MRI, of volume, texture, and intensity from tumor subregions are useful to understand the correlations with OS and gene expression. Six genes (TIMP1, C14orf39, EREG, ROS1, CHIT1, and WDR72) in GBM patients, with different levels of expression, were useful to develop radiomics-based prediction models discriminating patients in one of two categories, 1-year or less than 1 year survival time, achieving an accuracy of 81% with the GBDT algorithm [94]. In other work, a subset of 35-gene expression signature was selected to discriminate between rapidly-progressing and slowly-progressing patients, by using an SVM recursive feature elimination algorithm, where a $p < 0.05$ was obtained [95], tumors were predicted with low NF1 activity by using an ensemble of 500 LR classifiers and reporting a mean AUC of 0.77 [96], and the indicators OS, EGFR amplification, IDH mutation, Ki-67 expression, and MGMT methylation, were predicted by using Boruta algorithm for feature selection and XGBoost for classification, with the accuracy of 74%, 81%, 88%, 86%, and 71% respectively [97].

3.4.3. Characterization of Immunophenotypes

Immunophenotyping is the identification of the abundance of subpopulations of immune cells to estimate immune response. Characterization of immunophenotypes in GBM is important for therapeutic stratification and helps predict treatment response and prognosis. To classify G1 to G5 immunophenotypes of the GBM tumor microenvironment were employed the enrichment levels of aDC, Treg, cytotoxic T lymphocyte (CTL), and MDSC immune cells as features, together with radiomic characteristics from MRI and the RF algorithm. Using the T1-weighted contrast-enhanced imaging data, the average accuracies of the CTL, aDC, Treg, and MDSC models were 0.72, 0.75, 0.81, and 0.88, respectively. The rise of CTL infiltration in the GBM microenvironment demonstrated improvement in patients' survival by eliminating invasive tumor cells [98]. Single-cell phenotypes associated with continuous clinical variables were identified [99] through an unsupervised algorithm called Risk Assessment Population Identification (RAPID). This algorithm identifies five Glioblastoma Positive Prognostic clusters and four Glioblastoma Negative Prognostic clusters associated with OS. An average of 0.75 F-measure was reported for all clusters.

3.4.4. IDH Mutation

For predicting the IDH1 mutation status, the 1p/19q co-deletion status, and the grade of tumor, a single multi-task CNN that uses preoperative MRI scans was implemented. This is a non-invasive method that predicts multiple clinically relevant features of GBM. The CNN achieved an AUC of 0.90 for IDH1, 0.85 for 1p/19q co-deletion, and 0.81 for the grade (II/III/IV) [100].

The core signaling pathways in IDH wild-type GBM were predicted by using Next Generation Sequencing, perfusion, and diffusion MRI radiomics [101]. Radiogenomic feature selection was performed by t-tests, LASSO, and RF. The mixture between MRI phenotypes and clinical parameters improved the diagnosis compared with the use of only phenotypes obtained by MRI, achieving an AUC of 0.88. A model combining tumor core, whole tumor, edema, necrosis, enhancement, and non-enhancement was developed to preoperatively predict IDH1 mutation status in GBM. The ML techniques considered in this model are the RF classifier and all-relevant feature selector, achieving an accuracy of 97%. This radiomics-based classification with minimal MRI features allowed the prediction of IDH1 mutation in GBM [102].

4. DISCUSSION

Most of the works reviewed during the last 5 years (50%) focus on medical images to extract features through radiomics method, as illustrated in Fig. (4). The most used algorithms are LASSO for feature selection, and either RF or SVM for both classification and regression.

The most applied classical ML and DL methods within the different lines of research were compiled and classified in the diagram shown in Fig. (5). DL has seen greater use in recent years, due to the increase in computational power and because it allows us to skip the manual feature selection step. Also, it should be noted that ANNs have stood out for their presence

and use in tasks that required medical images. The problems that these methods addressed involve feature extraction,

segmentation, clustering, classification, and regression. The more relevant findings about the GBM problems tackled by ML methods are discussed in the following sections.

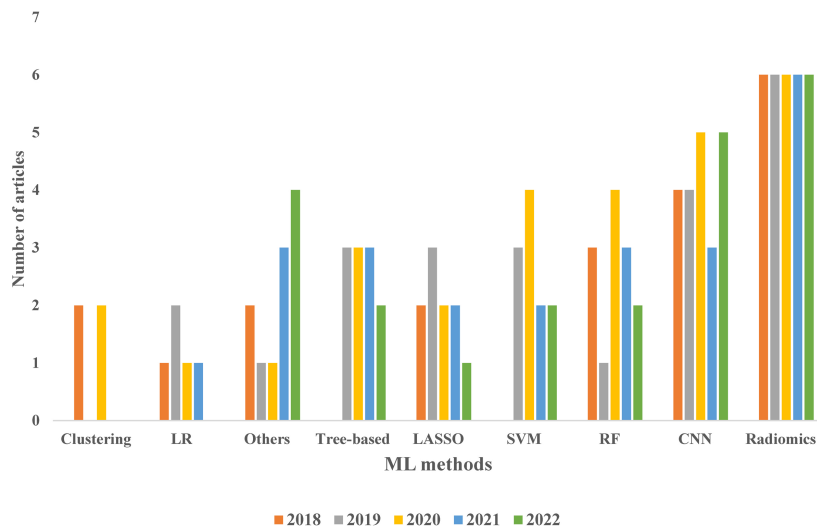


Fig. (4). ML techniques used in the works reviewed by year. CNN includes the architectures: ResNet-50 (2), VGG-19 (2), U-NET (2), MLP (3), VGG-16 (1), other CNNs architectures (6), and Transfer Learning (3). Clustering includes the methods: RAPID (1), Consensus (1), Hierarchical (2), and k-means (1). Other ML techniques were: Principal Components Analysis and Distance Correlation (1), Boruta (4), LDA (2), k-NN (2), and Naïve-Bayes. (2). Tree-based: GBDT (2), DT (3), and XGBoost (3). The number in parenthesis after the method or architecture indicates the articles in which was considered.

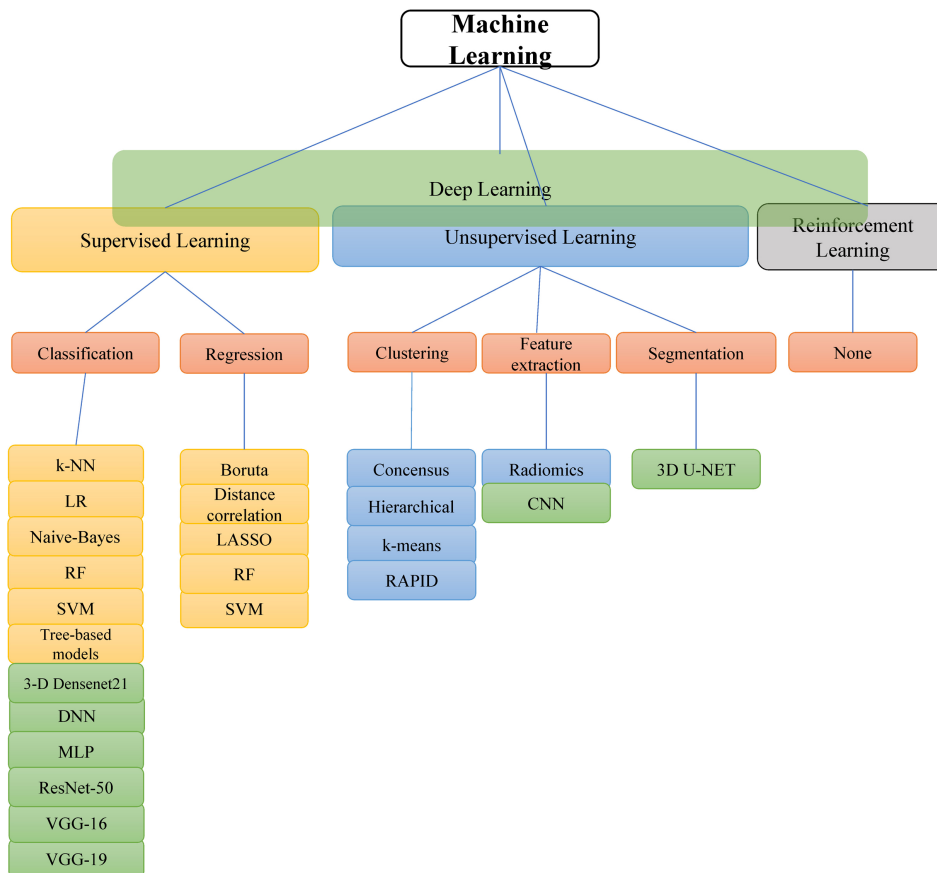


Fig. (5). ML taxonomy representing four learning approaches and their corresponding ML problems. Methods and architectures are grouped by ML problem. Most of the methods belong to the category of supervised learning to solve GBM classification problems, and the use of DL is appreciated in classification, feature extraction and segmentation (k-Nearest Neighbors (k-NN)).

4.1. GBM Problems

The GBM study can be divided into, at least, four main branches: I) feature extraction from different subregions, II) differentiation, III) characterization, and IV) genetic-based problems; and into 15 secondary branches: 1) edema, necrosis, enhancement, and tumor subregions, 2) METs, 3) AO, 4) PCNSL, 5) GSM, 6) multiple differentiation 7) subtypes, 8) TP vs PsP, 9) response to the treatment, 10) OS and PFS, 11) cellular density estimation, 12) prognostic of standard treatment, 13) survival outcome, 14) characterization of immunophenotypes, and 15) IDH mutation as illustrated in Fig. (3).

Features extraction: Regions such as edema, necrosis, enhancement, and the tumor were studied to find relationships with the evolution of the patient. There is a tendency to employ DL for tumor segmentation and radiomics techniques for feature extraction of GBM subregions. Applying ML algorithms to these extracted characteristics along with clinical, molecular, or biological data, a relationship was found between the tumor’s regions and the prognosis of the patient, its response to treatment, and survival. This information helps to build clinical nomograms for risk stratification, care implementation, and treatment selection. ML methods based on trees, like RF, reached an average accuracy of 93% in the problem of GBM subregions classification.

GBM differentiation: GBM was differentiated from five common brain tumors, METs, AO, PCNSL, meningioma and GSM. The most frequent differentiation problem was between GBM and METs. All reviewed works concluded that SVMs are those that better differentiate between GBM and other pathologies. The use of MRI and ML tools led to the discovery of characteristics to describe GBM, such as the manifestation of diffuse tumor cell infiltration, necrosis, or bleeding. SVMs reached accuracies up to 97% while more complicated algorithms like ResNet-50 only 88% in the GBM differentiation.

GBM characterization: The different GBM subtypes found in the review are proneural, mesenchymal, classical, and

neural. Relevant clinical findings suggest that the side where the tumor is located, and the progression pattern are important for the prognosis; also, variables such as age, MGMT status, and IDH1 were identified as indicators of patient survival time. Regarding ML models, ANN was important when differentiating TP vs PSP, the use of CNNs like U-Net for segmentation tasks, or ResNet-50 and VGG-16 for classification. In general, tree-related models such as XGBoost are easy to explain and apply in the clinic, reaching accuracies up to 88% in the subtypes classification problem. However, there are some problems like OS and response to the treatment that reached accuracies under 80% indicating that there is room for improvement.

Genetic-based problems: Survival prediction by using cancer gene expression, discrimination between rapid or slow progression, and classification of genes like IDH1 and MGMT, were among the tasks addressed by ML techniques. It was possible to predict IDH1 mutations and MGMT methylation preoperatively, this allows to reduce cost and risk to the patients. Unsupervised and DL models were broadly used to solve these problems. CNN architectures, clustering algorithms, and RF were the most used ML methods, achieving accuracy between 71% – 88%.

4.2. Machine Learning Methods

The most used methods, for classification, were SVM and RF, which obtained higher accuracy compared to other algorithms used in the same problem. LASSO was another relevant technique when making the selection of characteristics. Most of these articles focus on supervised learning, and a few address unsupervised learning problems, using clustering techniques, such as k-means.

It is worth mentioning that in these studies about GBM, the use of reinforcement learning was not found; however, algorithms from this ML category have been used in other clinical applications, such as in the mechanical evaluation and sedative dose in the intensive care area [2], and in the use for automated radiation adaptation [15].

Table 1. Summary of the analyzed studies working on the intersection between GBM problems and Machine Learning methods. The list of articles that consider each ML algorithm is sorted by GBM problem.

Machine Learning Algorithm	GBM Problems
	I. Feature extraction II. Differentiation III. Characterization IV. Genetic-based problems
CNN and other NNs	I [42, 103]. II [51, 60, 65]. III [66, 72, 73, 78, 79, 81, 83, 84, 87]. IV [89, 90, 92, 93, 100, 101, 102].
DT	III [66, 72, 74].
k-NN	III [72, 74]. IV [94].
LASSO	I [46]. II [54, 56, 59, 61]. III [84]. IV [89, 101].
LR	II [53, 55, 59]. IV [94, 96].
Radiomics	I [38, 42, 46, 48]. II [53, 55, 61]. III [66, 67, 69, 70, 75, 77, 78, 80, 81, 84]. IV [89, 91, 92, 94, 97, 98, 102].
Random Forest	I [42, 48, 49]. II [59, 63]. III [66, 70, 77, 85]. IV [92, 98, 101, 102].
SVM	I [44]. II [54, 56, 59, 61]. III [66, 69, 72, 82, 86]. IV [95].
XGBoost	II [59]. III [67]. IV [97].
Other algorithms	Boruta III [85]. IV [92, 97, 102]. Consensus IV [90]. GBDT II [56]. IV [94]. Hierarchical III [75]. IV [93]. LSIL I [104]. RAPID IV [99].

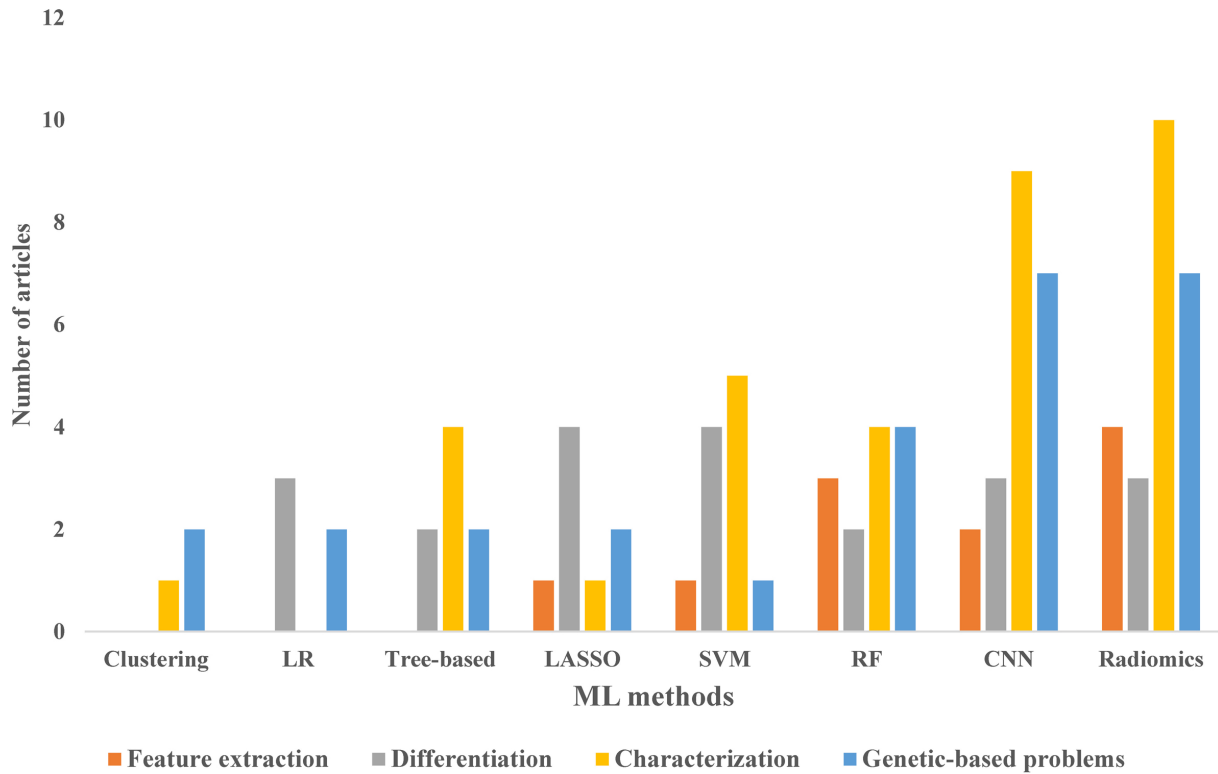


Fig. (6). Comparison between ML methods applied to the four GBM problems discussed in Table 1.

In addition to the identification of the best algorithms for each of the ML problems associated with glioblastoma (classification, segmentation, feature extraction, and clustering), the use of these algorithms in different GBM problems (feature extraction, differentiation, characterization, and genetic-based problems) is synthesized in Table 1 and illustrated in Fig. (6). There, it can be appreciated that Radiomics, RF, CNNs, SVM, and LASSO are the predominant ML methods applied in the analyzed studies.

4.2.1. Evaluation Metrics for ML Methods

Throughout the reviewed articles we can find different evaluation metrics according to the problems being addressed. The main metrics found are summarized in Table 2. As can be observed from this table, a given study may use a combination of metrics. For instance, Accuracy, AUC, S-S and p-value are used [61]; employed Accuracy, AUC, S-S, F-score [63]; in a study [90] only p-value is considered; or in another [38] Accuracy, AUC and C-index were applied. Each metric evaluates the result of the algorithm from a different perspective. Accuracy measures the fraction of cases that the

model correctly predicts. Sensitivity is how well a test identifies an abnormality and specificity is how well a test identifies normal patients. AUC measures how likely it is that the test will rank two patients: one with a lesion and one without, in the correct order, across all possible thresholds. C-index summarizes risk, event occurrence, and time in a single number that allows one to distinguish between good models and quasi-random ones. Moreover, p-value allows for comparison between groups.

4.3. Advantages and Limitations

In general, the advantages of ML methods include their capability to find complex relationships between a large number of input and target variables; their independence of human intervention to solve difficult work with high success ratio; their capability of handling multi-dimensional and multi-variety data, as well as to discover new trends and patterns. The main limitations of ML methods are their interpretability, the lack of metrics for their generalization capability, the potential bias due to their training with unbalanced data, and the privacy of patient data. Table 3 presents more advantages and limitations for specific ML methods.

Table 2. Evaluation metrics used in the reviewed articles.

Metrics	References
Accuracy	[38, 42, 44, 48, 49, 51, 53, 59, 60, 61, 62, 63, 65, 66, 67, 69, 70, 72, 73, 79, 80, 83, 89, 91, 92, 94, 97, 102]
AUC	[38, 49, 51, 53, 54, 56, 60, 61, 63, 69, 70, 72, 73, 74, 77, 78, 80, 82, 83, 92, 94, 96, 97, 100, 101, 102]
Sensitivity - Specificity (S-S)	[49, 51, 53, 61, 62, 63, 70, 73, 74, 79, 80, 83, 91]
C-index	[38, 46, 60, 70, 78, 101]
p-value	[61, 65, 69, 72, 75, 77, 78, 80, 81, 87, 90, 91, 94, 95, 96, 98, 99, 101]
Others	R ² [87, 88] F-score [63, 93, 102]

Table 3. Particular advantages and limitations of ML methods applied in GBM sub-problems.

Machine Learning Algorithm	Advantages	Disadvantages
CNN and other NNs	+ High reusability of pre-trained filters through transfer learning + Avoid manual extraction of characteristics	- Very low interpretability - Not pre-trained models require a large amount of data and specialized computational power
DT	+ High interpretability +It supports incremental learning	- Prone to overfitting and thus low generalization capability
k-NN	+ Works well on noisy data since it focuses on local neighborhoods. + Easy to implement	- Expensive computational costs - Lack of memory
LASSO	+ Works well with sparse data + Provides implicit variable selection.	- It is not generally path-consistent (the solution may not contain the true model, even if there is one)
LR	+ Easy to identify important predictors +Allows the calculation of confidence intervals	-Requires explicit modeling of interactions -Fails to detect complex relationships between input and output variables
Radiomics	+Ability to sample the whole tumor +Data can be extracted noninvasively using serial examinations	-The extracted image parameters relate to the macroscopic scale and are unlikely to bear a direct relationship to underlying cellular biology on a microscopic scale
Random Forest	+No need to specify the functional form and possible interactions +No rigid statistical assumptions about the distribution of the target variable +Tolerant of highly correlated predictors	-Requires the tuning of several hyperparameters -High sensitivity of predictions depending on the input data quality
SVM	+ High interpretability + Solid theory + Capable to provide a bound on the expected generalization performance based on the number of support vectors	- Expensive computational costs - Require specialized solvers for large datasets
XGBoost	+Eases the feature scoring +Does not require feature engineering (missing value imputation, scaling, etc.)	-Can overfit the data if hyperparameters are not adjusted correctly -It works only with numeric features

Most of the ML methods, and particularly all Neural Networks, work as black boxes after training. The underlying model is not interpretable by common users nor by specialists in computer sciences. Even for trained models with high performance, the lack of interpretability encumbers their implementation in clinical environments. Simple tree-based models like Decision Trees are the exception.

Concerning the generalization capability of the ML algorithms, only SVM possesses a metric based on the number of support vectors (the training instances required to build the model) to provide an estimate of generalization, the lesser the number of support vectors, the higher the generalization capability. The rest of the ML models could perform well on training data but provide unsatisfactory results on unseen cases. This raises the need for external evaluations of the trained models before being proposed as a computer-assisted diagnosis tool.

One more limitation is due to the availability of confirmed GBM cases. This implies that ML models are commonly trained with a higher number of negative cases, which adds an extra design problem that was not always considered in the review articles. Therefore, the ML model must be verified to be unbiased before being considered in medical practice.

Finally, the privacy of patient information represents one more limitation. This prevents private hospitals from sharing their data and their ML models. If private data could not be accessed, the reproducibility of successful methods would be limited.

FUTURE TRENDS

The application of DL methods on GBM problems is a noticeable trend that has grown exponentially in recent years. Except for SVM and RF algorithms which have remained among the most efficient. There is an exponentially increasing trend in the number of publications about ML in GBM. Adding 3730 DL and 5820 ML in 2022 compared to 297 DL and 1110 ML in 2017. Another trend is the increase in the availability of public databases, with open access to study these problems, such as the case of the UPenn described above (section 3.1) and The Cancer Genome Atlas Glioblastoma TCGA-GBM, The Cancer Imaging Archive, Ivy Glioblastoma Atlas known as IvyGAP, and REMBRANDT-VASARI. Since the tumor is highly lethal for the patient, any information that can be extracted from the analysis of these datasets with ML methods is valuable to improve patient survival. From all the papers reviewed, the use of MRI is still preferred to obtain GBM images rather than PET-CT probably due to its complexity and cost.

CONCLUSION

Four problems and 15 sub-problems associated with GBM handled with ML methods were identified and arranged in a partial taxonomy; several applications of ML methods were described for different purposes in the study of GBM, and the most successful were highlighted, thus achieving the objectives established in this work. In general, it is concluded that ML and DL methods are effective in solving GBM related

problems, with different precisions, the OS problem being the hardest to solve with an accuracy ranging from 57%-71%, and GBM differentiation the problem where ML methods achieved the highest accuracy ranging from 80% - 97%. In addition to accuracy, the evaluation metrics of sensitivity, specificity, AUC, C-index and p-value were found to be used either in combination or as a single measure depending on the ML method under consideration.

DL methods showed, in general, better performance than classic ML methods when applied to the same task; however, there are specific GBM problems such as the GBM differentiation, where the classic ML method SVM is preferred. Pre-trained convolutional DL networks stood out from the rest of ML methods as the state-of-the-art model in terms of performance; nonetheless, there is room for improvement in all the GBM sub-problems tackled with DL. There are still many other areas of research to be addressed such as the outcome of the combination of different treatments, the study of GBM using techniques of nuclear medicine, or GBM metabolism for diagnostic and prognostic. New categories of GBM problems and sub-problems are expected to be added to the proposed partial taxonomy due to the increasing number of investigations on GBM and ML. The results obtained by ML methods on different GBM problems motivate physicians to become interested in this modern technology.

LIST OF ABBREVIATIONS

ANN	= Artificial Neural Networks
AO	= Anaplastic Oligodendroglioma
AUC	= Area Under the Curve
CNN	= Convolutional Neural Networks
CTL	= cytotoxic T lymphocyte
DL	= Deep Learning
DT	= Decision Tree
EGFR	= epidermal growth factor receptor
GBDT	= Gradient Boost Decision Tree
GBM	= Glioblastoma
GSM	= Gliosarcoma
IDH	= Isocitrate dehydrogenase
k-NN	= k-Nearest Neighbors
LASSO	= Least Absolute Shrinkage and Selection Operator
LDA	= Linear Discriminant Analysis
LR	= Logistic Regression
METs	= Metastatic Brain Tumor
MGMT	= O6-Methylguanine-DNA Methyltransferase
ML	= Machine Learning
MLP	= Multilayer Perceptron
mpMRI	= multiparametric MRI
MRI	= Magnetic Resonance Imaging
OS	= Overall Survival
PCNSL	= Primary Central Nervous System Lymphoma
PFS	= Progression Free Survival

PsP	= Pseudoprogression
RAPID	= Risk Assessment Population Identification
ReLU	= Rectified Linear Unit
RF	= Random Forest
SVM	= Support Vector Machines
TCD	= Tumor Cell Density
TMZ	= Temozolomide

CONSENT FOR PUBLICATION

Not applicable.

STANDARDS OF REPORTING

PRISMA guidelines and methodology were followed.

AVAILABILITY OF DATA AND MATERIALS

The data and supportive information are available within the article.

FUNDING

This work was supported by the National Council of Science and Technology (CONACYT, Mexico), grant number 794494.

CONFLICT OF INTEREST

The authors declare no conflict of interest financial or otherwise.

ACKNOWLEDGEMENTS

Declared none.

SUPPLEMENTARY MATERIAL

PRISMA checklist is available as supplementary material on the publisher's website along with the published article.

Supplementary material is available on the publisher's website along with the published article.

REFERENCES

- [1] Bedrikovetski S, Dudi-Venkata NN, Maicas G, *et al.* Artificial intelligence for the diagnosis of lymph node metastases in patients with abdominopelvic malignancy: A systematic review and meta-analysis. *Artif Intell Med* 2021; 113: 102022. [<http://dx.doi.org/10.1016/j.artmed.2021.102022>] [PMID: 33685585]
- [2] Yu C, Ren G, Dong Y. Supervised-actor-critic reinforcement learning for intelligent mechanical ventilation and sedative dosing in intensive care units. *BMC Med Inform Decis Mak* 2020; 20(S3): 124. [<http://dx.doi.org/10.1186/s12911-020-1120-5>] [PMID: 32646412]
- [3] Shi F, Wang J, Shi J, *et al.* Review of artificial intelligence techniques in imaging data acquisition, segmentation, and diagnosis for COVID-19. *IEEE Rev Biomed Eng* 2021; 14: 4-15. [<http://dx.doi.org/10.1109/RBME.2020.2987975>] [PMID: 32305937]
- [4] Zhang L, Yu G, Xia D, Wang J. Protein-protein interactions prediction based on ensemble deep neural networks. *Neurocomputing* 2019; 324: 10-9. [<http://dx.doi.org/10.1016/j.neucom.2018.02.097>]
- [5] Nelson A, Herron D, Rees G, Nachev P. Predicting scheduled hospital attendance with artificial intelligence. *NPJ Digit Med* 2019; 2(1): 26. [<http://dx.doi.org/10.1038/s41746-019-0103-3>] [PMID: 31304373]
- [6] Reig B, Heacock L, Geras KJ, Moy L. Machine learning in breast MRI. *J Magn Reson Imaging* 2020; 52(4): 998-1018. [<http://dx.doi.org/10.1002/jmri.26852>] [PMID: 31276247]

- [7] Neromyliotis E, Kalamatianos T, Paschalis A, *et al.* Machine learning in meningioma MRI: Past to present. A narrative review. *J Magn Reson Imaging* 2022; 55(1): 48-60. [http://dx.doi.org/10.1002/jmri.27378] [PMID: 33006425]
- [8] Erickson BJ, Korfiatis P, Akkus Z, Kline TL. Machine learning for medical imaging. *Radiographics* 2017; 37(2): 505-15. [http://dx.doi.org/10.1148/rg.2017160130] [PMID: 28212054]
- [9] Gui C, Chan V. Machine learning in medicine. *Univ West Ont Med J* 2017; 86(2): 76-8. [http://dx.doi.org/10.5206/uwomj.v86i2.2060]
- [10] Ibrahim A, Gamble P, Jaroensri R, *et al.* Artificial intelligence in digital breast pathology: Techniques and applications. *Breast* 2020; 49: 267-73. [http://dx.doi.org/10.1016/j.breast.2019.12.007] [PMID: 31935669]
- [11] Lo Gullo R, Eskreis-Winkler S, Morris EA, Pinker K. Machine learning with multiparametric magnetic resonance imaging of the breast for early prediction of response to neoadjuvant chemotherapy. *Breast* 2020; 49: 115-22. [http://dx.doi.org/10.1016/j.breast.2019.11.009] [PMID: 31786416]
- [12] Gu D, Su K, Zhao H. A case-based ensemble learning system for explainable breast cancer recurrence prediction. *Artif Intell Med* 2020; 107: 101858. [http://dx.doi.org/10.1016/j.artmed.2020.101858] [PMID: 32828461]
- [13] Weis JA, Miga MI, Yankeelov TE. Three-dimensional image-based mechanical modeling for predicting the response of breast cancer to neoadjuvant therapy. *Comput Methods Appl Mech Eng* 2017; 314: 494-512. [http://dx.doi.org/10.1016/j.cma.2016.08.024] [PMID: 28042181]
- [14] Luo Y, McShan D, Ray D, *et al.* Development of a fully cross-validated bayesian network approach for local control prediction in lung cancer. *IEEE Trans Radiat Plasma Med Sci* 2019; 3(2): 232-41. [http://dx.doi.org/10.1109/TRPMS.2018.2832609] [PMID: 30854500]
- [15] Tseng HH, Luo Y, Cui S, Chien JT, Ten Haken RK, Naqa IE. Deep reinforcement learning for automated radiation adaptation in lung cancer. *Med Phys* 2017; 44(12): 6690-705. [http://dx.doi.org/10.1002/mp.12625] [PMID: 29034482]
- [16] Oerther B, Buren MV, Klein CM, Kirste S, Nicolay NH, Sprave T, *et al.* Predicting biochemical failure in irradiated patients with prostate cancer by tumour volume measured by multiparametric MRI. *In Vivo* 2020; 34(6): 3473-81. [http://dx.doi.org/10.21873/invivo.12187]
- [17] Valdes G, Simone CB II, Chen J, *et al.* Clinical decision support of radiotherapy treatment planning: A data-driven machine learning strategy for patient-specific dosimetric decision making. *Radiother Oncol* 2017; 125(3): 392-7. [http://dx.doi.org/10.1016/j.radonc.2017.10.014] [PMID: 29162279]
- [18] van Dijk LV, Van den Bosch L, Aljabar P, *et al.* Improving automatic delineation for head and neck organs at risk by Deep Learning Contouring. *Radiother Oncol* 2020; 142: 115-23. [http://dx.doi.org/10.1016/j.radonc.2019.09.022] [PMID: 31653573]
- [19] Ahn SH, Yeo AU, Kim KH, *et al.* Comparative clinical evaluation of atlas and deep-learning-based auto-segmentation of organ structures in liver cancer. *Radiat Oncol* 2019; 14(1): 213. [http://dx.doi.org/10.1186/s13014-019-1392-z] [PMID: 31775825]
- [20] Fechter T, Adebahr S, Baltas D, Ben Ayed I, Desrosiers C, Dolz J. Esophagus segmentation in CT via 3D fully convolutional neural network and random walk. *Med Phys* 2017; 44(12): 6341-52. [http://dx.doi.org/10.1002/mp.12593] [PMID: 28940372]
- [21] Jung JW, Lee C, Mosher EG, *et al.* Automatic segmentation of cardiac structures for breast cancer radiotherapy. *Phys Imaging Radiat Oncol* 2019; 12: 44-8. [http://dx.doi.org/10.1016/j.phro.2019.11.007] [PMID: 33458294]
- [22] Chao HH, Valdes G, Luna JM, *et al.* Exploratory analysis using machine learning to predict for chest wall pain in patients with stage I non-small-cell lung cancer treated with stereotactic body radiation therapy. *J Appl Clin Med Phys* 2018; 19(5): 539-46. [http://dx.doi.org/10.1002/acm2.12415] [PMID: 29992732]
- [23] Hasnain Z, Mason J, Gill K, *et al.* Machine learning models for predicting post-cystectomy recurrence and survival in bladder cancer patients. *PLoS One* 2019; 14(2): e0210976. [http://dx.doi.org/10.1371/journal.pone.0210976] [PMID: 30785915]
- [24] Lombardi M, Assem M. Glioblastoma genomics: A very complicated story. In: *Glioblastoma*. Brisbane (AU): Codon Publications 2017. [http://dx.doi.org/10.15586/codon.glioblastoma.2017.ch1]
- [25] Valdebenito J, Medina F. Machine learning approaches to study glioblastoma: A review of the last decade of applications. *Cancer Rep* 2019; 2(6): e1226. [http://dx.doi.org/10.1002/cnr2.1226] [PMID: 32729254]
- [26] Nguyen AV, Blears EE, Ross E, Lall RR, Ortega-Barnett J. Machine learning applications for the differentiation of primary central nervous system lymphoma from glioblastoma on imaging: A systematic review and meta-analysis. *Neurosurg Focus* 2018; 45(5): E5. [http://dx.doi.org/10.3171/2018.8.FOCUS18325] [PMID: 30453459]
- [27] Neil ZD, Pierzchajlo N, Boyett C, *et al.* Assessing metabolic markers in glioblastoma using machine learning: A systematic review. *Metabolites* 2023; 13(2): 161. [http://dx.doi.org/10.3390/metabo13020161] [PMID: 36837779]
- [28] Booth TC, Grzeda M, Chelliah A, *et al.* Imaging biomarkers of glioblastoma treatment response: A systematic review and meta-analysis of recent machine learning studies. *Front Oncol* 2022; 12: 799662. [http://dx.doi.org/10.3389/fonc.2022.799662] [PMID: 35174084]
- [29] Tewarie IA, Senders JT, Kremer S, *et al.* Survival prediction of glioblastoma patients—are we there yet? A systematic review of prognostic modeling for glioblastoma and its clinical potential. *Neurosurg Rev* 2021; 44(4): 2047-57. [http://dx.doi.org/10.1007/s10143-020-01430-z] [PMID: 33156423]
- [30] Uribe CF, Mathotaarachchi S, Gaudet V, *et al.* Machine learning in nuclear medicine: Part 1—Introduction. *J Nucl Med* 2019; 60(4): 451-8. [http://dx.doi.org/10.2967/jnumed.118.223495] [PMID: 30733322]
- [31] Zukotynski K, Gaudet V, Uribe CF, *et al.* Machine learning in nuclear medicine: Part 2—neural networks and clinical aspects. *J Nucl Med* 2021; 62(1): 22-9. [http://dx.doi.org/10.2967/jnumed.119.231837] [PMID: 32978286]
- [32] Young RJ, Knopp EA. Brain MRI: Tumor evaluation. *J Magn Reson Imaging* 2006; 24(4): 709-24. [http://dx.doi.org/10.1002/jmri.20704] [PMID: 16958058]
- [33] Nehring S, Tadi P, Tenny S. Cerebral Edema. *StatPearls Publishing* 2022.
- [34] Gillies RJ, Kinahan PE, Hricak H. Radiomics: Images are more than pictures, they are data. *Radiology* 2016; 278(2): 563-77. [http://dx.doi.org/10.1148/radiol.2015151169] [PMID: 26579733]
- [35] van Timmeren JE, Cester D, Tanadini-Lang S, Alkadhi H, Baessler B. Radiomics in medical imaging—“how-to” guide and critical reflection. *Insights Imaging* 2020; 11(1): 91. [http://dx.doi.org/10.1186/s13244-020-00887-2] [PMID: 32785796]
- [36] Tian J, Dong D, Liu Z, Wei J. *Radiomics and Its Clinical Application*. China: Academic Press 2021.
- [37] Moradmand H, Aghamiri SMR, Ghaderi R. Impact of image preprocessing methods on reproducibility of radiomic features in multimodal magnetic resonance imaging in glioblastoma. *J Appl Clin Med Phys* 2020; 21(1): 179-90. [http://dx.doi.org/10.1002/acm2.12795] [PMID: 31880401]
- [38] Cepeda S, Pérez-Núñez A, García-García S, *et al.* Predicting short-term survival after gross total or near total resection in glioblastomas by machine learning-based radiomic analysis of preoperative MRI. *Cancers* 2021; 13(20): 5047. [http://dx.doi.org/10.3390/cancers13205047] [PMID: 34680199]
- [39] Leung K. Naive bayesian classifier. In: *Polytechnic University Department of Computer Science/Finance and Risk Engineering*. 2007; pp. 123-56.
- [40] Siddique N, Paheding S, Elkin CP, Devabhaktuni V. U-net and its variants for medical image segmentation: A review of theory and applications. *IEEE Access* 2021; 9(9): 82031-57. [http://dx.doi.org/10.1109/ACCESS.2021.3086020]
- [41] Mitchell R, Frank E. Accelerating the XGBoost algorithm using GPU computing. *PeerJ Comput Sci* 2017; 3: e127. [http://dx.doi.org/10.7717/peerj-cs.127]
- [42] Shboul ZA, Alam M, Vidyaratne L, Pei L, Elbakary MI, Iftekaruddin KM. Feature-guided deep radiomics for glioblastoma patient survival prediction. *Front Neurosci* 2019; 13(966): 966. [http://dx.doi.org/10.3389/fnins.2019.00966] [PMID: 31619949]
- [43] Noble WS. What is a support vector machine? *Nat Biotechnol* 2006; 24(12): 1565-7. [http://dx.doi.org/10.1038/nbt1206-1565] [PMID: 17160063]
- [44] Ye Z, Price RL, Liu X, *et al.* Diffusion histology imaging combining diffusion basis spectrum imaging (DBSI) and machine learning improves detection and classification of glioblastoma pathology. *Clin Cancer Res* 2020; 26(20): 5388-99. [http://dx.doi.org/10.1158/1078-0432.CCR-20-0736] [PMID: 32694155]
- [45] Lemhadri I, Ruan F, Abraham L, Tibshirani R. LassoNet: A neural network with feature sparsity. *J Mach Learn Res* 2021; 22: 1-29.

- [46] Yang Y, Han Y, Hu X, *et al.* An improvement of survival stratification in glioblastoma patients *via* combining subregional radiomics signatures. *Front Neurosci* 2021; 15: 683452. [http://dx.doi.org/10.3389/fnins.2021.683452] [PMID: 34054424]
- [47] Cha Z, Yunqian M. *Ensemble Machine Learning: Methods and Applications*. Springer 2012; pp. 157-76. [http://dx.doi.org/10.1007/978-1-4419-9326-7_5]
- [48] Chiu FY, Le NQK, Chen CY. A multiparametric MRI-based radiomics analysis to efficiently classify tumor subregions of glioblastoma: A pilot study in machine learning. *J Clin Med* 2021; 10(9): 2030. [http://dx.doi.org/10.3390/jcm10092030] [PMID: 34068528]
- [49] Chiu FY, Yen Y. Efficient radiomics-based classification of multiparametric MR images to identify volumetric habitats and signatures in glioblastoma: A machine learning approach. *Cancers* 2022; 14(6): 1475. [http://dx.doi.org/10.3390/cancers14061475] [PMID: 35326626]
- [50] Bakas S, Sako C, Akbari H, *et al.* The University of Pennsylvania glioblastoma (UPenn-GBM) cohort: Advanced MRI, clinical, genomics, & radiomics. *Sci Data* 2022; 9(1): 453. [http://dx.doi.org/10.1038/s41597-022-01560-7]
- [51] Shin I, Kim H, Ahn SS, *et al.* Development and validation of a deep learning-based model to distinguish glioblastoma from solitary brain metastasis using conventional MR images. *AJNR Am J Neuroradiol* 2021; 42(5): 838-44. [http://dx.doi.org/10.3174/ajnr.A7003] [PMID: 33737268]
- [52] LaValley MP. Logistic Regression. *Circulation* 2008; 117(18): 2395-9. [http://dx.doi.org/10.1161/CIRCULATIONAHA.106.682658] [PMID: 18458181]
- [53] Chen C, Ou X, Wang J, Guo W, Ma X. Radiomics-based machine learning in differentiation between glioblastoma and metastatic brain tumors. *Front Oncol* 2019; 9: 806. [http://dx.doi.org/10.3389/fonc.2019.00806] [PMID: 31508366]
- [54] Qian Z, Li Y, Wang Y, *et al.* Differentiation of glioblastoma from solitary brain metastases using radiomic machine-learning classifiers. *Cancer Lett* 2019; 451: 128-35. [http://dx.doi.org/10.1016/j.canlet.2019.02.054] [PMID: 30878526]
- [55] de Causans A, Carré A, Roux A, *et al.* Development of a machine learning classifier based on radiomic features extracted from post-contrast 3D T1-Weighted MR images to distinguish glioblastoma from solitary brain metastasis. *Front Oncol* 2021; 11: 638262. [http://dx.doi.org/10.3389/fonc.2021.638262] [PMID: 34327133]
- [56] Fan Y, Chen C, Zhao F, *et al.* Radiomics-based machine learning technology enables better differentiation between glioblastoma and anaplastic oligodendroglioma. *Front Oncol* 2019; 9(1164): 1164. [http://dx.doi.org/10.3389/fonc.2019.01164] [PMID: 31750250]
- [57] Ke G, Meng Q, Finley T, Wang T, Chen W. Lightgbm: A highly efficient gradient boosting decision tree. *Adv Neural Inf Process Syst* 2017; 30.
- [58] Xanthopoulos P, Pardalos P, Trafalis T. Linear discriminant analysis. In: *Robust Data Mining*. Springer 2013; pp. 27-33. [http://dx.doi.org/10.1007/978-1-4419-9878-1_4]
- [59] Chen C, Zheng A, Ou X, Wang J, Ma X. Comparison of radiomics-based machine-learning classifiers in diagnosis of glioblastoma from primary central nervous system lymphoma. *Front Oncol* 2020; 10(1151): 1151. [http://dx.doi.org/10.3389/fonc.2020.01151] [PMID: 33042784]
- [60] Xia W, Hu B, Li H, *et al.* Deep learning for automatic differential diagnosis of primary central nervous system lymphoma and glioblastoma: Multi-parametric magnetic resonance imaging based convolutional neural network model. *J Magn Reson Imaging* 2021; 54(3): 880-7. [http://dx.doi.org/10.1002/jmri.27592] [PMID: 33694250]
- [61] Qian Z, Zhang L, Hu J, *et al.* Machine learning-based analysis of magnetic resonance radiomics for the classification of gliosarcoma and glioblastoma. *Front Oncol* 2021; 11: 699789. [http://dx.doi.org/10.3389/fonc.2021.699789] [PMID: 34490097]
- [62] Shrot S, Salhov M, Dvorski N, Konen E, Averbuch A, Hoffmann C. Application of MR morphologic, diffusion tensor, and perfusion imaging in the classification of brain tumors using machine learning scheme. *Neuroradiology* 2019; 61(7): 757-65. [http://dx.doi.org/10.1007/s00234-019-02195-z] [PMID: 30949746]
- [63] Stadlbauer A, Marhold F, Oberndorfer S, *et al.* Radiophysiomics: Brain tumors classification by machine learning and physiological mri data. *Cancers* 2022; 14(10): 2363. [http://dx.doi.org/10.3390/cancers14102363] [PMID: 35625967]
- [64] Ramchoun H, Idrissi MAJ, Ghanou Y, Ettaouil M. Multilayer perceptron: Architecture optimization and training. *Reunir* 2017; 71: 1-6. [http://dx.doi.org/10.1145/3090354.3090427]
- [65] Swinburne NC, Schefflein J, Sakai Y, *et al.* Machine learning for semi-automated classification of glioblastoma, brain metastasis and central nervous system lymphoma using magnetic resonance advanced imaging. *Ann Transl Med* 2019; 7(11): 232. [http://dx.doi.org/10.21037/atm.2018.08.05] [PMID: 31317002]
- [66] Wijethilake N, Islam M, Meedeniya D, Chitraranjan C, Perera I, Ren H. Radiogenomics of glioblastoma: Identification of radiomics associated with molecular subtypes. *Lect Notes Comput Sci* 2020; 12449: 229-39. [http://dx.doi.org/10.1007/978-3-030-66843-3_22]
- [67] Le K, Do T, Dang L, Huynh T-T. Radiomics-based machine learning model for efficiently classifying transcriptome subtypes in glioblastoma patients from MRI. *Comput Biol Med* 2021; 132: 104320. [http://dx.doi.org/10.1016/j.compbiomed.2021.104320]
- [68] Le Fèvre C, Lhermitte B, Ahle G, *et al.* Pseudoprogression *versus* true progression in glioblastoma patients: A multiapproach literature review. *Crit Rev Oncol Hematol* 2021; 157: 103188. [http://dx.doi.org/10.1016/j.critrevonc.2020.103188] [PMID: 33307200]
- [69] Akbari H, Rathore S, Bakas S, *et al.* Histopathology-validated machine learning radiographic biomarker for noninvasive discrimination between true progression and pseudo-progression in glioblastoma. *Cancer* 2020; 126(11): 2625-36. [http://dx.doi.org/10.1002/cncr.32790] [PMID: 32129893]
- [70] Sun YZ, Yan LF, Han Y, *et al.* Differentiation of pseudoprogression from true progression in glioblastoma patients after standard treatment: A machine learning strategy combined with radiomics features from T₁-weighted contrast-enhanced imaging. *BMC Med Imaging* 2021; 21(1): 17. [http://dx.doi.org/10.1186/s12880-020-00545-5] [PMID: 33535988]
- [71] Kingsford C, Salzberg SL. What are decision trees? *Nat Biotechnol* 2008; 26(9): 1011-3. [http://dx.doi.org/10.1038/nbt0908-1011] [PMID: 18779814]
- [72] Yan JL, Toh CH, Wei KC, Chen PY. A neural network approach to identify glioblastoma progression phenotype from multimodal MRI. *Cancers* 2021; 13(9): 2006. [http://dx.doi.org/10.3390/cancers13092006]
- [73] Moassefi M, Faghani S, Conte GM, *et al.* A deep learning model for discriminating true progression from pseudoprogression in glioblastoma patients. *J Neurooncol* 2022; 159(2): 447-55. [http://dx.doi.org/10.1007/s11060-022-04080-x] [PMID: 35852738]
- [74] Geldof T, Van Damme N, Huys I, Van Dyck W. Patient-level effectiveness prediction modeling for glioblastoma using classification trees. *Front Pharmacol* 2020; 10: 1665. [http://dx.doi.org/10.3389/fphar.2019.01665] [PMID: 32116674]
- [75] Li Z, Wang Y, Yu J, Guo Y, Zhang Q. Age groups related glioblastoma study based on radiomics approach. *Comput Assist Surg* 2017; 22(sup1): 18-25. [http://dx.doi.org/10.1080/24699322.2017.1378722] [PMID: 28914549]
- [76] Sabel M. Principles of adjuvant chemotherapy for breast cancer. In: *Essentials of Breast Surgery*. Mosby 2009; pp. 247-66. [http://dx.doi.org/10.1016/B978-0-323-03758-7.00016-8]
- [77] Bae S, Choi YS, Ahn SS, *et al.* Radiomic MRI phenotyping of glioblastoma: Improving survival prediction. *Radiology* 2018; 289(3): 797-806. [http://dx.doi.org/10.1148/radiol.2018180200] [PMID: 30277442]
- [78] Yoon HG, Cheon W, Jeong SW, *et al.* Multi-parametric deep learning model for prediction of overall survival after postoperative concurrent chemoradiotherapy in glioblastoma patients. *Cancers* 2020; 12(8): 2284. [http://dx.doi.org/10.3390/cancers12082284] [PMID: 32823939]
- [79] Wankhede DS, Selvarani R. Dynamic architecture based deep learning approach for glioblastoma brain tumor survival prediction. *Neurosci Inf* 2022; 2(4): 100062. [http://dx.doi.org/10.1016/j.neuri.2022.100062]
- [80] Osman AFI. A multi-parametric MRI-based radiomics signature and a practical ML model for stratifying glioblastoma patients based on survival toward precision oncology. *Front Comput Neurosci* 2019; 13(58): 58. [http://dx.doi.org/10.3389/fncom.2019.00058] [PMID: 31507398]
- [81] Han W, Qin L, Bay C, *et al.* Deep transfer learning and radiomics feature prediction of survival of patients with high-grade gliomas.

- AJNR Am J Neuroradiol 2020; 41(1): 40-8.
[<http://dx.doi.org/10.3174/ajnr.A6365>] [PMID: 31857325]
- [82] Xin J, Yixuan Z, Dixiang S, *et al.* A multiparametric MRI-based radiomics nomogram for preoperative prediction of survival stratification in glioblastoma patients with standard treatment. *Front Oncol* 2022; 12: 758622.
[<http://dx.doi.org/10.3389/fonc.2022.758622>]
- [83] Jajroudi M, Enferadi M, Homayoun AA, Reiazi R. MRI-based machine learning for determining quantitative and qualitative characteristics affecting the survival of glioblastoma multiforme. *Magn Reson Imaging* 2022; 85: 222-7.
[<http://dx.doi.org/10.1016/j.mri.2021.10.023>] [PMID: 34687850]
- [84] Lao J, Chen Y, Li ZC, *et al.* A deep learning-based radiomics model for prediction of survival in glioblastoma multiforme. *Sci Rep* 2017; 7(1): 10353.
[<http://dx.doi.org/10.1038/s41598-017-10649-8>] [PMID: 28871110]
- [85] Della Pepa GM, Caccavella VM, Menna G, *et al.* Machine learning-based prediction of 6-month postoperative karnofsky performance status in patients with glioblastoma: Capturing the real-life interaction of multiple clinical and oncologic factors. *World Neurosurg* 2021; 149: e866-76.
[<http://dx.doi.org/10.1016/j.wneu.2021.01.082>] [PMID: 33516864]
- [86] Lamichhane B, Daniel AGS, Lee JJ, Marcus DS, Shimony JS, Leuthardt EC. Machine learning analytics of resting-state functional connectivity predicts survival outcomes of glioblastoma multiforme patients. *Front Neurol* 2021; 12(64224): 642241.
[<http://dx.doi.org/10.3389/fneur.2021.642241>] [PMID: 33692747]
- [87] Hu LS, Yoon H, Eschbacher JM, *et al.* Accurate patient-specific machine learning models of glioblastoma invasion using transfer learning. *AJNR Am J Neuroradiol* 2019; 40(3): 418-25.
[<http://dx.doi.org/10.3174/ajnr.A5981>] [PMID: 30819771]
- [88] Gates EDH, Weinberg JS, Prabhu SS, *et al.* Estimating local cellular density in glioma using MR imaging data. *AJNR Am J Neuroradiol* 2021; 42(1): 102-8.
[<http://dx.doi.org/10.3174/ajnr.A6884>] [PMID: 33243897]
- [89] Wong KK, Rostomily R, Wong STC. Prognostic gene discovery in glioblastoma patients using deep learning. *Cancers* 2019; 11(1): 53.
[<http://dx.doi.org/10.3390/cancers11010053>] [PMID: 30626092]
- [90] Young JD, Cai C, Lu X. Unsupervised deep learning reveals prognostically relevant subtypes of glioblastoma. *BMC Bioinformatics* 2017; 18(S11): 381.
[<http://dx.doi.org/10.1186/s12859-017-1798-2>] [PMID: 28984190]
- [91] Do DT, Yang MR, Lam LHT, Le NQK, Wu YW. Improving MGMT methylation status prediction of glioblastoma through optimizing radiomics features using genetic algorithm-based machine learning approach. *Sci Rep* 2022; 12(1): 13412.
[<http://dx.doi.org/10.1038/s41598-022-17707-w>] [PMID: 35927323]
- [92] Li ZC, Bai H, Sun Q, *et al.* Multiregional radiomics features from multiparametric MRI for prediction of MGMT methylation status in glioblastoma multiforme: A multicentre study. *Eur Radiol* 2018; 28(9): 3640-50.
[<http://dx.doi.org/10.1007/s00330-017-5302-1>] [PMID: 29564594]
- [93] Choi S, Cho HH, Koo H, Cho K, Nanning KH. Multi-habitat radiomics unravels distinct phenotypic subtypes of glioblastoma with clinical and genomic significance. *Cancers* 2020; 12(7): 1707.
[<http://dx.doi.org/10.3390/cancers12071707>]
- [94] Xin L, Bo C, Bin T. Machine-learning based radiogenomics analysis of MRI features and metagenes in glioblastoma multiforme patients with different survival time. *J Cell Mol Med* 2019; 23(6): 4375-85.
[<http://dx.doi.org/10.1111/jcmm.14328>]
- [95] Fatai AA, Gamielien J. A 35-gene signature discriminates between rapidly- and slowly-progressing glioblastoma multiforme and predicts survival in known subtypes of the cancer. *BMC Cancer* 2018; 18(1): 377.
[<http://dx.doi.org/10.1186/s12885-018-4103-5>] [PMID: 29614978]
- [96] Way GP, Allaway RJ, Bouley SJ, Fadul CE, Sanchez Y, Greene CS. A machine learning classifier trained on cancer transcriptomes detects NF1 inactivation signal in glioblastoma. *BMC Genomics* 2017; 18(1): 127.
[<http://dx.doi.org/10.1186/s12864-017-3519-7>] [PMID: 28166733]
- [97] Pasquini L, Napolitano A, Lucignani M, Tagliente E, Dellepiane F, Rossi-Espagnet MC, *et al.* Comparison of machine learning classifiers to predict patient survival and genetics of GBM: Towards a standardized model for clinical implementation. *cornell university. arXiv:210206526* 2021.
- [98] Hsu JBK, Lee GA, Chang TH, *et al.* Radiomic immunophenotyping of gsea-assessed immunophenotypes of glioblastoma and its implications for prognosis: A feasibility study. *Cancers* 2020; 12(10): 3039.
[<http://dx.doi.org/10.3390/cancers12103039>] [PMID: 33086550]
- [99] Leelatian N, Sinnaeve J, Mistry AM, *et al.* Unsupervised machine learning reveals risk stratifying glioblastoma tumor cells. *eLife* 2020; 9: e56879.
[<http://dx.doi.org/10.7554/eLife.56879>] [PMID: 32573435]
- [100] Voort S, Incekara F, Wijnenga M, *et al.* Combined molecular subtyping, grading, and segmentation of glioma using multi-task deep learning. *Neuro-Oncology* 0000; 25(2): 279-89.
[<http://dx.doi.org/10.1093/neuonc/noac166>]
- [101] Park JE, Kim HS, Park SY, *et al.* Prediction of core signaling pathway by using diffusion- and perfusion-based mri radiomics and next-generation sequencing in isocitrate dehydrogenase wild-type glioblastoma. *Radiology* 2020; 294(2): 388-97.
[<http://dx.doi.org/10.1148/radiol.2019190913>] [PMID: 31845844]
- [102] Li ZC, Bai H, Sun Q, *et al.* Multiregional radiomics profiling from multiparametric MRI: Identifying an imaging predictor of IDH1 mutation status in glioblastoma. *Cancer Med* 2018; 7(12): 5999-6009.
[<http://dx.doi.org/10.1002/cam4.1863>] [PMID: 30426720]
- [103] Wu J, He S, Zhou S. Multi-atlas subcortical segmentation: An orchestration of 3D fully convolutional network and generalized mixture function. *Mach Vis Appl* 2023; 34(4): 64.
[<http://dx.doi.org/10.1007/s00138-023-01415-0>]
- [104] Wu J, Yang Q, Zhou S. Latent shape image learning *via* disentangled representation for cross-sequence image registration and segmentation. *Int J CARS* 2022; 18(4): 621-8.
[<http://dx.doi.org/10.1007/s11548-022-02788-9>] [PMID: 36346499]

